

**Immobilization of natural lipid biomembranes and their interactions with choline carboxylates.
A Nanoplasmonic sensing study**

Filip Duša,¹ Wen Chen,² Joanna Witos,³ Antti H. Rantamäki,² Alistair W. T. King,² Evangelos Sklavounos,^{2, 4} Michal Roth,¹ Susanne K. Wiedmer^{*2}

¹Institute of Analytical Chemistry of the Czech Academy of Sciences, v. v. i., Veveří 97, 602 00 Brno, Czech Republic

²Department of Chemistry, A.I. Virtasen aukio 1, P.O. Box 55, FI-00014 University of Helsinki, Finland

³Department of Bioproducts and Biosystems, P.O. Box 11000, FI-00076 AALTO, Aalto University Finland

⁴Neste Engineering Solutions Oy, P.O. Box 310, FI-06101, Porvoo, Finland

Correspondence: Dr. Susanne K. Wiedmer: susanne.wiedmer@helsinki.fi

ORCID:

0000-0001-5219-2153 (FD)

0000-0002-3027-1763 (WC)

0000-0003-0021-1599 (JW)

0000-0001-8490-6069 (AHR)

0000-0003-3142-9259 (AWTK)

0000-0003-3212-1467 (ES)

0000-0001-9147-3863 (MR)

0000-0002-3097-6165 (SKW)

Keywords:

natural lipid biomembrane; choline carboxylate; nanoplasmonic sensing; interaction; ionic liquid; immobilization

Abstract

The cell membrane is mainly composed of lipid bilayers with inserted proteins and carbohydrates. Lipid bilayers made of purified or synthetic lipids are widely used for estimating the effect of target compounds on cell membranes. However, the composition of such biomimetic membranes is much simpler than the composition of biological membranes. Interactions between compounds and simple composition biomimetic membranes might not demonstrate the effect of target compounds as precisely as membranes with compositions close to real organisms. Therefore, the aim of our study is to construct biomimetic membrane closely mimicking the state of natural membranes. Liposomes were prepared from lipids extracted from L- α -phosphatidylcholine, *Escherichia coli*, yeast (*Saccharomyces cerevisiae*) and bovine liver cells through agitation and sonication. They were immobilized onto SiO₂ sensor surfaces using N-(2-hydroxyethyl)piperazine-N'-2-ethanesulfonic acid buffer with calcium chloride. The biomimetic membranes were successfully immobilized onto the SiO₂ sensor surface and detected by nanoplasmonic sensing. The immobilized membranes were exposed to choline carboxylates. The membrane disruption effect was, as expected, more pronounced with increasing carbohydrate chain length of the carboxylates. The results correlated with the toxicity values determined using *Vibrio fischeri* bacteria. The yeast extracted lipid membranes had the strongest response to introduction of choline laurate while the bovine liver lipid extracted liposomes were the most sensitive towards the shorter choline carboxylates. This implies that the composition of the cell membrane plays a crucial role upon interaction with choline carboxylates, and underlines the necessity of testing membrane systems of different origin to obtain an overall image of such interactions.

1 Introduction

The cell membrane separates the interior of the cell from the external environment and only certain components can enter into the cell through this semi-permeable membrane using either passive or active transport. One important function of the cell membrane is to prevent the invasion of toxic compounds. The structure of the cell membrane is composed of a lipid bilayer with embedded proteins and carbohydrates.

The lipids in the cell membrane are categorized into three types: phospholipids, glycolipids, and sterols. Among them, phospholipids are the most abundant in most cells. They form a bilayer structure and offer a barrier to the surrounding medium. Based on this, simplified biomimetic membranes composed of phospholipid bilayers are commonly used to model interaction mechanisms of cell membranes with target compounds [1–5]. Phospholipids can be processed into unilamellar vesicles through extrusion or sonication. They can further be immobilized onto sensing surfaces as a supported lipid bilayer (SLB) or as an intact supported vesicle layer (SVL), depending on the surface material and the immobilization conditions [6,7]. Since phosphatidylcholine (PC) is found in most cell membranes, it is by far the most commonly used phospholipid in biomimetic membrane studies. Typical long-alkyl-chain PCs used in studies are combination of saturated and unsaturated alkyl chains 1-palmitoyl-2-oleoyl-*sn*-glycero-3-phosphocholine (POPC) and saturated 1,2-dipalmitoyl-*sn*-glycero-3-phosphocholine (DPPC) [8,9].

In addition to phospholipids, sterols are also important lipids which contribute to the fluidity of the cell membrane. In animal cells, cholesterol is the most abundant sterol. Hence, cholesterol has also been included in biomimetic membranes [10]. Our recent study showed that the inclusion of cholesterol in PC liposomes affected the interactions between liposomes and an ionic liquid (IL), methyltrioctylphosphonium acetate ([P₈₈₈₁][OAc]) [11]. Increase of the cholesterol proportion reduced the IL-induced depletion of lipids from the liposomes. This result not only demonstrates that the introduction of cholesterol to the membrane hinders lipid removal but also indicates that the composition of biomimetic membranes strongly influences their interactions with target compounds. Therefore, it would be beneficial to use biomimetic membranes with compositions similar to the real cell membrane. This gives a better understanding on how target compounds interact with cell membranes.

Recently, we successfully immobilized liposomes with a composition very similar to the cell membrane of *Escherichia coli* (*E. coli*) [12], when a total lipid extract from *E. coli* was used for the membrane preparation. The liposomes were immobilized onto silicon dioxide (SiO₂)-coated sensors using sodium N-(2-hydroxyethyl)piperazine-N'-2-ethane sulfonate (Na-HEPES) buffer containing calcium chloride (Ca-HEPES). In this study, we immobilized phospholipids extracted from yeast (*Saccharomyces cerevisiae*), *i.e.*, eukaryotic cells, and bovine liver cells for comparison against the immobilization of egg PC and *E. coli* liposomes. Since the combination of Na-HEPES and calcium ions was found to be crucial for liposome immobilization on fused silica capillaries and SiO₂ coated sensors [13,14], the same pretreatment was applied to immobilize the natural liposomes in this work. One of the aims in this study was to obtain biomimetic membranes with lipid compositions very similar to natural cellular membranes and to firmly immobilize them onto the sensor surface.

After obtaining the biomimetic membranes (SLBs or SVLs), we further applied them to study interactions with choline-based ILs (choline carboxylates). Choline carboxylates have high potential of application in biomass industry as novel environmental friendly molecular solvents [15,16]. Carboxylates are also ubiquitous in nature and industry due to their surfactant and hydrotropic properties. However, before applying them widely in industry, it is important to understand their cytotoxicity [17]. Biomembranes constructed from liposomes were previously used to investigate the effect of ILs on cells [18,19]. It has been demonstrated that the cytotoxicity of choline

carboxylates increases as the alkyl chain length increases; the longer the alkyl chain length the stronger was the influence of the choline carboxylates on model lipid bilayers, as revealed by differential scanning microcalorimetry [20]. The compositions of the membranes in cells are far more complicated than those of homogeneous lipid bilayers. Therefore, to get a better understanding on how choline carboxylates affect cell membranes, it is essential to apply biomimetic membranes with compositions similar to natural cell membranes. The choline carboxylates chosen for this study included choline laurate, choline decanoate, choline octanoate, and choline hexanoate, as shown in Figure 1.

The immobilization of liposomes composed of natural lipids and their interactions with choline carboxylates were investigated by nanoplasmonic sensing (NPS). NPS is an optical technique based on localized surface plasmon resonance (LSPR) [21,22]. One of the main advantages of the techniques is that it is a label-free method [23]. On the sensor chip, gold nanodiscs with an approximate diameter of 120 nm are well separated and coated by a thin layer of SiO₂. Adsorption of vesicles on the sensing surface causes a change in the dielectric environment in close proximity to the nanodiscs. This change is manifested by a redshift in the maximum extinction wavelength (λ_{\max}) and the shift of λ_{\max} is subsequently detected as an NPS signal. Since NPS is a highly sensitive technique for investigating liposome properties, it has been used for studying the immobilization of liposomes [24–26] and their interactions with target compounds [6,11].

In this study, we demonstrate that liposomes composed of natural lipids can successfully be immobilized on a SiO₂ coated sensor surface, using Ca-HEPES buffer in the pretreatment. The immobilization was monitored and recorded utilizing NPS. Furthermore, we show that the interactions between choline carboxylates and the biomimetic membranes vary a lot, depending on the composition of the membrane. This emphasizes the crucial role of the composition of biomimetic membranes in studying interactions between compounds and biomimetic membranes.

2 Materials and Methods

2.1 Chemicals

L- α -phosphatidylcholine in chloroform (egg PC, 840051C), *E. coli* total lipid extract in chloroform (product number (PN) 100500), yeast total lipid extract (*Saccharomyces cerevisiae*) in chloroform (PN 190000C) and bovine liver total lipid extract (*Bos taurus*) in chloroform (PN 181104C) were purchased from Avanti Polar Lipids (Alabaster, AL, USA). The lipid compositions of the studied membranes are summarized in Table 1 (data obtained from the manufacturer, Avanti Polar Lipids). 2-[4-(2-hydroxyethyl)piperazin-1-yl]ethanesulfonic acid was from Sigma (Darmstadt, Germany) and sodium hydroxide pellets were from J.T. Baker Chemicals (Center Valley, PA, USA). Calcium chloride was purchased from VWR International OY (Espoo, Finland) and HPLC grade methanol was from Fischer Chemical (Fisher scientific, Loughborough, U.K.). MilliQ water was obtained by purification of distilled water using a Millipore water purification system (Millipore, Molsheim, France). *Vibrio fischeri* bacteria and the chemicals for the Microtox assay were from Modern Water (Guildford, UK). Sodium chloride was from Fisher Chemical (Fisher scientific, Loughborough, U.K.).

2.2 Synthesis of choline carboxylates

Choline carboxylates, including choline laurate, choline decanoate, choline octanoate, and choline hexanoate were synthesized at the Department of Chemistry at the University of Helsinki. The synthesis and characterization of choline decanoate [19] and choline hexanoate [27] have been described in our previous studies. For choline laurate, the synthesis protocol was as follows. Lauric acid (5 g, 0.0250 mol) was added to a round bottom flask, methanol (5 mL) was added and the solution was mixed to dissolve the acid. Choline hydroxide (3.03 g of dry weight of the salt, 7.13 mL of 45 wt% solution in methanol at a density of 0.945 g/mL) was added and the solution was mixed until homogeneous. Methanol was then evaporated in a rotary evaporator to yield a gel-like solid, after relaxation. The final product was determined to be pure, except for a trace of methanol (3.38 ppm in the ^1H NMR spectrum) which amounted to less than 1 wt% (Supporting material Figure S1). A similar protocol was applied to synthesize choline octanoate. Instead of lauric acid, octanoic acid (5 g, 0.0347 mol) was added. The amount of choline hydroxide was 4.21 g dry weight, 9.90 mL of 45 wt% solution in methanol at a density of 0.945 g/mL. Methanol was evaporated to yield a glassy liquid, after relaxation. The final product was determined to be pure, except for a trace of methanol (3.37 ppm in the ^1H NMR spectrum) which amounted to less than 1 wt% (Supporting material Figure S2).

Table 1. Lipid compositions of extracts from *E. coli*, yeast (*Saccharomyces cerevisiae*), and bovine liver.

	<i>E. coli</i> extract (wt/wt %)	Yeast^a extract (wt/wt %)	Bovine liver extract (wt/wt %)
Anionic (-)	PG ^c (15.1) CL ^d (9.8)	PI ^f (13.29) PS ^g (4.41) PA ^h (1.06) PG (0.51)	PI (8) Lyso PI (1)
Zwitterionic	PE ^e (57.5)	PC (18.74) PE (4.51) Lyso PE (1.91) Lyso PC (0.56) GPC ⁱ (0.05)	PC (42) PE (22)
Less polar			Cholesterol (7) Other (20), incl. neutral lipids
Unknown	17.6	0.33	

^a For yeast lipid extract, the amount of phospholipids is only 45.37 wt% of total mass.
^b phosphatidylcholine; ^c phosphatidylglycerol; ^d cardiolipin; ^e phosphatidylethanol;
^f phosphatidylinositol; ^g phosphatidylserine; ^h phosphatidic acid; ⁱ glycerophosphocholine

2.3 Buffer preparation

Na-HEPES buffer solution with an ionic strength of 10 mM and a pH value adjusted to 7.4 ± 0.05 was used throughout the study. The Na-HEPES buffer solution was filtered through a 0.45 μm filter (Gelman Sciences, Ann Arbor, MI, USA). The Na-HEPES buffer containing 5 mM CaCl_2 (Ca-HEPES) was prepared by mixing with an appropriate amount of 0.5 M CaCl_2 in Na-HEPES buffer solution.

2.4 Cytotoxicity of choline carboxylates

Vibrio fischeri bacteria were exposed to at least four different choline carboxylate concentrations in 2% (w/v) sodium chloride solution. By recording the time and concentration dependent decay of the bioluminescence, the median effective concentrations (EC50) values were determined at set time intervals of 5 and 15 min using a Microtox 500 luminometer/thermostate apparatus (Modern Water, USA). Two independent measurements were performed for each IL as duplicates.

2.5 Critical micelle concentrations of choline carboxylates

To determine the critical micelle concentrations (CMCs), we applied the optical pendant drop method with a contact angle meter (CAM 200, KSV Instruments, Espoo, Finland). The CMC determination protocol has been described in detail [19]. The CMCs of choline decanoate [19] and choline hexanoate [27] have been measured in our previous studies. In this study, we determined the CMCs of choline laurate and choline octanoate.

2.6 Liposome preparation

The preparations of egg PC and *E. coli* liposomes have been described previously in detail [12,28]. To prepare yeast liposomes, 400 μL of yeast lipid extract in chloroform (25 mg/mL) was added to a test tube. Chloroform was evaporated under a gentle flow of air and to remove traces of chloroform. The test tube with the lipid extract was kept in a desiccator under vacuum overnight. The lipid film was rehydrated in 2 mL of Na-HEPES buffer solution in order to obtain a 5 mg/mL yeast lipid extract dispersion. The solution was shaken (Biosan, TS-100 Thermo Shaker, Riga, Latvia) at a speed of 800 RPM at 60 °C for 1 hour to obtain a dispersion of multilamellar vesicles (MLVs). The yeast lipid MLVs were further processed to smaller size vesicles by sonicating them in a bath

sonicator (Elmasonic P, Elma, Singen, Germany) for 20 min at a frequency of 37 kHz (power of 100%). The temperature of the sonication bath was kept at 35 °C. The yeast lipid extract dispersion was filtered through a 0.45 µm PVDF syringe filter (B. Braun, Inject-F, Melsungen, Hessen, Germany). After filtration, the dispersion was kept at 4 °C. The same vesicle preparation steps were applied to obtain bovine liver liposome stock dispersions. The stock vesicle dispersions (5 mg/mL) were diluted to 0.11 mg/mL in Na-HEPES or Ca-HEPES buffer before measurement. The size distributions of the prepared vesicles were determined by a Zetasizer Nano ZS instrument (Malvern Instruments, Malvern, Worcestershire, U.K.). The prepared vesicle solutions were measured 7 times, and each consisted of 12 to 15 repetitions. The average vesicle sizes (based on volume distribution) of egg PC, *E. coli*, yeast, and bovine liver liposomes were 31 ± 3 nm, 33 ± 2 nm, 51 ± 11 nm, and 48 ± 9 nm, respectively.

2.7 NPS measurement

The NPS measurements were conducted with an Insplorion XNano II instrument (Insplorion AB, Gothenburg, Sweden). The instrument setup has previously been described in detail [6]. In this study, we applied SiO₂-coated sensors. Before the first measurement, the sensor was pretreated for 20 min with oxygen plasma, using an UV ozone cleaner (UVC-1014 NanoBioAnalytics, Berlin, Germany). Between each measurement, the sensor was immersed in methanol and cleaned in a sonication bath for 5 min (sweeping mode, frequency of 80 kHz and power of 30 %). After sonication, the sensor was dried with a gentle stream of compressed air. The quality of the used SiO₂ sensor was confirmed by the bulk refractive index (RI) sensitivity of 104.75 nm per RI unit (Supporting material Figure S3). All NPS measurements were performed twice to ensure the repeatability of the recorded peak shift curves.

2.8 Immobilization of liposomes

The immobilization of egg PC and *E. coli* liposomes was conducted according to our previous research [12,28]. Briefly, water was rinsed through the measurement cell until a stable signal of peak shift ($\Delta\lambda$) was obtained. The measurement itself started with a 5 min rinse with water, Na-HEPES buffer, and Ca-HEPES buffer. The rinsing was followed by direct introduction of the liposome dispersion until a stable $\Delta\lambda$ was reached, indicating saturation of the sensor surface.

For the immobilization of yeast and bovine liver liposomes, water was first flushed into the measurement chamber for 5 min to obtain a stable signal. After that, the sensor was subsequently rinsed for 5 min with Na-HEPES and Ca-HEPES buffers. Next, yeast liposomes were diluted to 0.11 mg/mL with 5 mM Ca-HEPES and were introduced to the measurement chamber, until a stable signal was achieved. The same protocol was also applied for the immobilization of bovine liver liposomes. After that, Ca-HEPES buffer, Na-HEPES buffer, and water were introduced successively to investigate the stability of liposome immobilization on the SiO₂ coated sensor surface.

2.9 Interactions between choline carboxylates and the SiO₂ sensor surface

The reference (blank) signal of the four studied choline carboxylates on the SiO₂ sensor was investigated. The sensor was first pretreated with water (3 min), then Ca-HEPES (3 min) and finally water (5 min). This sensor pretreatment was followed by the introduction of the choline carboxylates until a stable $\Delta\lambda$ was obtained. After that, the sensor was rinsed again with water and the change in the $\Delta\lambda$ was recorded. This procedure was performed for all four choline carboxylates.

2.10 Interactions between liposomes and choline carboxylates

The sensor was first flushed with water (3 min), then Ca-HEPES buffer (3 min), followed by the introduction of the liposomes. When a stable signal was reached, the sensor was flushed with Ca-HEPES buffer, Na-HEPES buffer

and then water, just before introducing the choline carboxylates. The studied choline carboxylate was introduced and changes in the $\Delta\lambda$ were recorded. When the signal became stable, the sensor was rinsed with water. The measurement ended when the $\Delta\lambda$ reached a plateau value.

2.11 Analysis of interactions between liposomes and choline carboxylates by curve fitting

An exponential curve fitting model was utilized for description of the obtained NPS $\Delta\lambda$ over time of the interacting systems. The fitted function was

$$y = A_1 + e^{(A_2 - A_3 \cdot x)} \quad (1)$$

where y is the peak shift and x is the time. The parameters A_1 , A_2 , and A_3 were calculated using the nonlinear optimization routine of the KyPlot 5.0 software [29]. The parameter A_1 determines the vertical shift (horizontal asymptote) of the exponential curve. This parameter predicts the value of the $\Delta\lambda$ at which the system change levels out, *i.e.*, the new stable value of the $\Delta\lambda$ after the interaction system reaches equilibrium. The parameter A_2 marks the horizontal shift of the exponential curve. This parameter is closely related to the time point at which the exponential decrease of the $\Delta\lambda$ occurred. Both parameters A_1 and A_2 are strictly related to the position of the exponential curve in the graph and do not change the shape of the exponential function. In contrast, the parameter A_3 is connected to the steepness of the exponential curve. The higher is the value of A_3 the steeper is the drop of the exponential curve. This relates parameter A_3 directly to the initial decrease rate of the $\Delta\lambda$ caused by introduction of the IL. In this regard it can be connected to the rate of the interaction of the IL with the established SLB/SVL system. Strong correlation can be expected for parameters A_2 and A_3 due to the direct connection of the parameters in the exponential expression. Therefore, the parameters A_1 and A_3 should be the most important for the description of the obtained NPS data curves. Depending on the data and connected quality of the fit, a few fitting attempts were completed and the one with the lowest residual sum of squares value was selected and used for the description of the interacting system.

3 Results and discussion

3.1 Immobilization of liposomes

According to the methods set up in our previous studies, egg PC and *E. coli* liposomes were immobilized onto NPS sensors coated with SiO₂ [12,28]. An initial drop in the $\Delta\lambda$ (blueshift) was observed at the beginning of the liposome introduction, indicating that there was adsorption of larger vesicles in the beginning of the immobilization [30]. Since the liposomes were prepared by sonication, the size distribution was broader compared to that obtained by extrusion. Also, the liposome size obtained after sonication strongly suggests that the resulting diameter is affected by the membrane lipid composition. Hence, in addition to small unilamellar vesicles (SUVs), there might have been a low number of large vesicles in the liposome dispersion. This results in an initial blueshift, as larger vesicles scatter lower wavelengths more than higher wavelengths due to the (wave vector)⁴ dependence for the scattering cross section. Such scattering results in the detection of blueshift of the peak maximum in transmitted light. The total $\Delta\lambda$ for complete immobilization of egg PC and *E. coli* liposomes was 3.5 nm (Figure 2A and 2B). At a threshold point of sensor surface saturation with vesicles, the egg PC liposomes began to break and formed an SLB. This was indicated by the $\Delta\lambda$ time derivative curve (inset of Figure 2A), which showed a $\Delta\lambda$ increase rate acceleration at around 16 min. Calcium ions usually work as strong fusogenic agents, promoting the formation of SLBs [31]. However, immobilization of *E. coli* liposomes with Ca-HEPES resulted in the formation of vesicle aggregates and their adsorption was slow. When calcium cations from Ca-HEPES were exchanged to sodium by the introduction of Na-HEPES solution, the aggregates started to disassemble, and part of the released vesicles adsorbed on a free part of the SiO₂ surface to form a layer of intact vesicles on the sensor surface (SVL). The observed adsorption and its mechanism are described in detail in our previous work [12]. Therefore, while the egg PC and *E. coli* had similar hydrodynamic diameters, their adsorption paths were completely different due to the differences in the lipid composition.

The time to reach the plateau level for yeast liposomes was much longer (20 min) than for bovine liver liposomes (7 min) (Figures 2C and 2D). The slower adsorption rate of the yeast liposomes compared to bovine liver liposomes is probably due to the higher negative surface charge of the yeast vesicles, which is caused by a higher concentration of negatively charged lipids (see Table 1). Since the sensor in this study was coated with SiO₂, which is negatively charged at pH 7.4, electric charge repulsion will be more pronounced during adsorption and, therefore, it will take a longer time for the yeast liposomes to cover the surface to complete saturation. When the sensor surface was saturated with liposomes, a $\Delta\lambda$ plateau value was reached. The final $\Delta\lambda$ for yeast and bovine liver liposomes were both approximately 5.2 nm, which implies high saturation coverage on the sensor surface in both cases. Furthermore, a similar pattern of the $\Delta\lambda$ time derivative curve (inset of Figure 2) has been observed by Zan *et al.*, who linked this pattern to the adsorption of intact vesicles onto a titanium oxide coated sensor [32]. This supports our observation that the yeast and bovine liver liposomes remain in the form of intact vesicles and form SVLs upon immobilization on the SiO₂ sensor surface.

The sensor covered with the SVL was subsequently flushed with buffer solutions (Ca-HEPES and Na-HEPES) and water to provide reference $\Delta\lambda$ for further evaluation of the changes caused by the interacting ionic liquids. Due to differences in the refractive index of the background solutions, a small change in the $\Delta\lambda$ was observed. However, the initial change was followed by a stable peak-shift that signaled that the SLB/SVL remained intact.

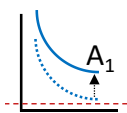
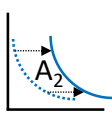
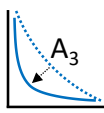
3.2 Interactions between choline carboxylates and the SiO₂ sensor surface

Next, the interactions between the four choline carboxylates and the SiO₂ sensor surface were studied. Reference runs were conducted on choline carboxylates, in order to obtain basic information about possible interactions

between the chosen ILs and the SiO₂ coated sensor. The concentrations of the IL solutions were selected based on their EC₅₀ values. The EC₅₀ values of the choline carboxylates with 5 min incubation were determined by assessing their cytotoxicity towards *Vibrio fischeri* bacterial cells, and the obtained values were 4.4 ± 0.2 mM for choline hexanoate [27], 0.46 ± 0.02 mM for choline octanoate, 0.10 ± 0.02 mM for choline decanoate [19], and 0.045 ± 0.006 mM for choline laurate. The EC₅₀ values with 15 min incubation were almost the same as after 5 min incubation. This suggests that the toxic effect takes place rapidly, *i.e.*, during the first 5 min of incubation. According to a mass concentration based classification, choline hexanoate and choline octanoate are practically harmless (100-1000 mg/L), while choline decanoate and choline laurate are moderately toxic (10-100 mg/L) [33]. Our previous research has shown that in order to observe the deformation of liposomes in NPS, much higher IL concentrations than the corresponding EC₅₀ values were required [6,11]. In regard to those findings, the concentrations of carboxylate based ILs studied in this work were chosen accordingly: 20 mM of choline laurate, 50 mM of choline decanoate, 200 mM of choline octanoate, and 200 mM of choline hexanoate. Figures 3A-D demonstrates that the introduction of choline carboxylates to the bare sensor lead to an increase in the $\Delta\lambda$; 1.2, 2.9, 3.2 and 1.3 nm $\Delta\lambda$ was detected for choline laurate, choline decanoate, choline octanoate and choline hexanoate, respectively.

During the subsequent water rinse, the $\Delta\lambda$ of all four choline carboxylates dropped gradually. This indicates that the choline carboxylates were only weakly adsorbed and gradually rinsed off the SiO₂ surface. At the end of the water rinse (5-10 min), the $\Delta\lambda$ of choline laurate and choline decanoate returned to the $\Delta\lambda$ level before the introduction of the choline carboxylates, while choline octanoate and choline hexanoate remained 0.4 nm and 0.3 nm above this level. The parameter A_f value, determining the stable value of the $\Delta\lambda$ after the interaction system reaches equilibrium, ranged from -0.04 to 0.03 for all the carboxylates (see Table 2 and Figure 3A-D). This suggests that all the carboxylates have negligible interaction with the SiO₂ surface and the NPS $\Delta\lambda$ returned to the initial $\Delta\lambda$ value. The rate at which the ILs' $\Delta\lambda$ dropped during rinse with water (A_3) was higher with the shorter alkyl chain lengths of the carboxylates (see Table 2). However, this could be influenced by the different concentrations of the applied choline carboxylates.

Table 2. Analysis of interactions between liposomes and choline carboxylates by curve fitting. Parameters A_1 and A_2 are strictly related to the position of the exponential curve in the graph and do not change the shape of the exponential function (the parameter A_1 determines the vertical shift while the parameter A_2 marks the horizontal shift of the exponential curve). The parameter A_3 is connected to the steepness of the exponential curve (the higher is the value of A_3 the steeper is the drop).

Exponential function fitting of NPS interaction analysis					
$y = A_1 + e^{(A_2 - A_3 \cdot x)}$					
System label	A_1	A_2	A_3	Residual Sum of Squares	Coefficient of Determination
					
ILs reference NPS					(Figure 3)
20 mM choline laurate	-0.04	4.5	0.015	0.02	0.98
50 mM choline decanoate	-0.03	4.7	0.016	0.02	0.98
200 mM choline octanoate	0.01	8.4	0.025	0.01	0.99
200 mM choline hexanoate	0.03	7.8	0.021	0.02	0.98
egg PC SLB with					(Figure 4)
0.5 mM choline laurate	fitting not succesful				
5 mM choline laurate	fitting not succesful				
20 mM choline laurate	2.21	33.5	0.034	0.91	0.98
20 mM choline laurate with					(Figure 5)
<i>Escherichia coli</i> SVL	1.25	117.7	0.032	1.43	0.99
Yeast exctrat SVL 1st drop	1.11	28.1	0.017	3.49	0.98
Yeast exctrat SVL 2nd drop	-0.35	10.9	0.005	3.94	0.92
Liver extract SVL	2.39	31.5	0.031	1.01	0.99
egg PC SLB with					(Figure 6)
20 mM choline decanoate	fitting not succesful				
50 mM choline decanoate 1st drop	3.21	18.3	0.015	0.83	0.97
50 mM choline decanoate 2nd drop	2.12	17.3	0.010	0.07	0.99
105 mM choline decanoate 1st drop	1.33	105.9	0.089	0.04	0.99
105 mM choline decanoate 2nd drop	-0.25	46.9	0.033	2.41	0.95
50 mM choline decanoate with					(Figure 7)
<i>Escherichia coli</i> SVL	fitting not succesful				
Yeast exctrat SVL 1st drop	3.02	34.0	0.022	1.43	0.98
Yeast exctrat SVL 2nd drop	2.63	32.8	0.018	0.17	0.98
Liver extract SVL 1st drop	3.05	22.3	0.021	1.06	0.98
Liver extract SVL 2nd drop	2.03	20.0	0.014	1.01	0.97
egg PC SLB with					(Figure 8)
50 mM choline octanoate	fitting not succesful				
200 mM choline octanoate 1st drop	3.16	24.8	0.024	0.376	0.98
200 mM choline octanoate 2nd drop	1.52	2.3	0.002	0.025	1.00
200 mM choline octanoate with					(Figure 9)
<i>Escherichia coli</i> SVL	fitting not succesful				
Yeast exctrat SVL	3.141	51.9	0.037	2.434	0.97
Liver extract SVL 1st drop	3.188	27.2	0.025	1.419	0.96
Liver extract SVL 2nd drop	3.608	13.6	0.010	0.053	0.98
200 mM choline hexanoate with					(Figure 10)
egg PC SLB	fitting not succesful				
<i>Escherichia coli</i> SVL	fitting not succesful				
Yeast exctrat SVL	fitting not succesful				
Liver extract SVL	4.609	46.5	0.035	0.020	0.99

3.3 Interactions between choline carboxylates and lipid membranes

Introduction of egg PC liposomes resulted in a formation of a SLB on the sensor. After a short water rinse (5 min), choline laurate was introduced onto the immobilized SLB of egg PC. Three different concentrations of choline

laurate (0.5, 5 and 20 mM) were chosen for this study (Figure 4). The EC50 value of choline laurate was 0.045 mM meaning that all studied concentrations were above the toxicity value. In addition, CMC of choline laurate was 13 ± 0.1 mM. Two of the concentrations, *i.e.*, 0.5 and 5 mM, were below the CMC, indicating that all choline laurate was in the solution as unimers. However, at 20 mM concentration, which was above the CMC, part of the choline laurate was present in an aggregated micellar form. Upon addition of 0.5 mM of choline laurate to the liposome coated sensor, the $\Delta\lambda$ changed almost negligibly (0.2 nm; Figure 4A). This could be caused by partitioning of unimers of choline laurate into the SLB. A similar phenomenon of surfactant partitioning into the vesicle bilayer has been shown by López et al. [34]. During the following water rinsing step, no change in the $\Delta\lambda$ was detected which supports that the partitioned unimers of choline laurate remained within the SLB.

When the concentration of choline laurate was increased to 5 mM, a small increase in the $\Delta\lambda$ was observed at the beginning of the IL introduction, that was closely followed by a $\Delta\lambda$ drop, which reached a value of 0.4 nm within 5 min of IL application. (Figure 4B). It can be expected that the partitioning of unimers of choline laurate into the SLB continued with the increased IL concentration and the molar ratio of IL in the SLB increased accordingly. A subsequent water rinse first induced a positive $\Delta\lambda$ (1.1 nm), and then the signal started to decrease slowly to reach the $\Delta\lambda$ level of original SLB. Such behavior was not seen during analysis of interaction of egg PC SLB with surfactants studied in our previous work [28]. Therefore, it is hard to predict the outcomes of the interaction. Nevertheless, the system seemed to return to the stable state close to the initial SLB so it suggests there were no significant changes in the refractive index of SLB caused by interaction with unimers of choline laurate. Due to the small changes of $\Delta\lambda$, exponential fitting with the concentrations 0.5 and 5 mM was not successful.

Application of choline laurate micelles (20 mM) to the SLB of egg PC liposomes coated onto the sensor resulted in a faster ($A_3 = 0.034$) and larger drop (-2.5 nm, $A_I = 2.21$) in the $\Delta\lambda$ (Figure 4C and Table 2), compared to application of 5 mM choline laurate. NPS data suggest that IL micelles were able to incorporate into SLB with high efficiency. Subsequently, we observed an immediate and large increase in the $\Delta\lambda$ (3.0 nm). One of the possible explanations might be partial detachment of SLB from SiO₂ surface with increasing incorporation of choline laurate micelles. Water rinse probably caused the formed IL-SLB to attach back, however the integrity of the mixed system was lower than that of the original SLB and the IL-SLB system was slowly rinsed out of the sensor surface signaled by the linear decrease of the $\Delta\lambda$ (Figure 4C).

We chose 20 mM choline laurate for further investigation of its interaction with three SVLs composed of natural lipids because of the strongest NPS response obtained with the egg PC SLB. It should be noted that in the case of SVL the IL interacted with vesicles instead of lipid bilayers. Vesicles with their susceptibility to rupture or change shape/curvature and planar bilayers are different systems in regard to possible interactions with surfactant ILs. The difference between the egg PC SLB and egg PC SVL interaction was studied in our recent work [28]. The findings obtained there were used to explain the observed interaction effect in connection to the supported lipid form where it was applicable.

For immobilized *E. coli* liposomes, the introduction of choline laurate induced a large drop in the $\Delta\lambda$ (-3.3 nm; $A_I = 1.25$; $A_3 = 0.032$; Figure 5A). Most probably choline laurate partitioned into the *E. coli* vesicles, resulting in solubilisation and detachment of the *E. coli* vesicles. The A_3 value of 0.032 suggests a high rate of partitioning. The subsequent water rinse lowered the concentration of choline laurate and, hence, the vesicle removal process stopped. Additionally, it seems that a new lipid structure rich in choline laurate was formed on the sensor surface, as suggested by an increase in the $\Delta\lambda$ (1.1 nm). A continuous decrease in the $\Delta\lambda$ (Figure 5A) can be interpreted as instability and a slow removal of the mixed system from the sensor surface.

For yeast and bovine liver liposomes both $\Delta\lambda$ dropped significantly after the introduction of choline laurate (Figure 5B and 5C). The rate of the $\Delta\lambda$ drop was slower with yeast SVL ($A_3 = 0.017$) while the bovine liver SVL showed a similar rate ($A_3 = 0.031$) as *E. coli* SVL. This indicates immediate partitioning of choline laurate into the SVLs connected with the removal of phospholipid-choline laurate aggregates from the sensor surface. Upon a subsequent water flush, only a small spike was observed, suggesting an abrupt change in the immobilized surface. Further the signal continued with a slower drop ($A_3 = 0.005$ for yeast SVL), implying continuing removal of the SVLs enriched with choline laurate from the sensor surface.

3.4 Interaction between choline decanoate and lipid membranes

Three different concentrations of choline decanoate (20, 50, and 105 mM) were first tested on egg PC liposomes (Figure 6). It has been shown previously, that compounds with shorter alkyl chains have less effect on liposomes [20]. 20 mM, 50 mM, and 105 mM concentrations of the choline decanoate were selected for NPS analysis. The two higher concentrations were above the CMC value (23 ± 4 mM) of the IL [19]. After introduction of 20 mM of choline decanoate, a small decrease of 0.5 nm was observed (Figure 6A). During the water rinse the $\Delta\lambda$ increased slightly above the original level of the SLB in water. This suggests that choline decanoate unimers were not able to penetrate deeper into the SLB, the IL was gradually washed out, and the SLB rearranged to a conformation close to its original. Additionally, compared to 20 mM choline laurate, the effect of the same concentration of choline decanoate on egg PC liposome was much weaker. This is consistent with previous studies, which have shown that the shorter the alkyl chain, the smaller is the effect on liposomes and the lower is the toxicity [19,20,35].

The introduction of 50 mM and 105 mM of choline decanoate micelles to the SLBs induced a large $\Delta\lambda$ drop of 1.7 nm and 3.2 nm, respectively (Figure 6B and 6C). Rates of the $\Delta\lambda$ decrease (A_3) were 0.15 and 0.89 for 50 mM and 105 mM IL, respectively. This indicates formation of a mixed system of IL-egg PC with rate depending on the concentration of IL. A sharp spike in the $\Delta\lambda$ was observed when water was introduced to the SLB after the IL treatment (observed at both IL micellar concentrations). This suggests that upon introduction of water, the mixed system goes under a transient state where it briefly increases contact with the surface probably by rearrangement of IL-enriched SLB over the surface with free spots caused by partial solubilisation. However, at the same time, the stability of such a system is not strong enough and the mixed system is removed from the SLB (A_3 parameters of 0.010 and 0.033 for 50 and 105 mM IL respectively). The value of parameter A_1 (2.12) suggests that with the addition of 50 mM of choline decanoate the developed system remained on the surface, while 105 mM of choline decanoate showed complete removal of the SLB ($A_1 = -0.025$). These results suggest that the formed SLB-IL systems strongly depends on the ratio of choline decanoate and phospholipids. The increasing portion of choline decanoate results in weaker adsorption to the SiO₂ surface. 50 mM concentration was used for the interaction studies with the SVLs made of natural lipids.

After addition of 50 mM choline decanoate to *E. coli*, yeast and bovine liver SVL (Figure 7A-C), we obtained very similar patterns to the SLBs of egg PC. A fast drop in the $\Delta\lambda$ was observed with all three SVLs (A_3 0.022 (yeast) and 0.021 (bovine liver)), made of natural lipids, indicating removal of phospholipids from the SVL. In addition, the decrease in the signals was similar; 2.7, 2.9 and 2.6 nm for *E. coli*, yeast and bovine liver liposomes, respectively. Subsequent water rinse again followed the pattern known from egg PC analysis. Such behavior of the IL versus different supported biomembrane structures suggests that the formed mixed system is mostly composed of the choline decanoate which dictates its main features. While in minor amount, phospholipids probably play important role of the stabilization of IL-SVL system on SiO₂ surface as the 50 mM choline decanoate itself is not able to develop any supported layer (see Figure 3B).

3.5 Interaction between choline octanoate and lipid membranes

50 and 200 mM choline octanoate interaction with egg PC was investigated (Figure 8A-B). The concentrations were selected in regard to the CMC of choline octanoate of 78 ± 2 mM. At 50 mM concentration, no $\Delta\lambda$ changes were observed after addition of IL and subsequent water rinse (Figure 8A). This observation is similar to the choline decanoate where unimers at 20 mM concentration were not able to partition into the SLB layer. Significant effect was observed with 50 mM choline decanoate which was already above CMC. When the choline octanoate concentration was increased to 200 mM a 1.5 nm drop in the $\Delta\lambda$ was observed ($A_I = 3.16$; $A_3 = 0.024$), suggesting that phospholipids were partly solubilized by micelles and egg PC SLB was partly mixed with choline octanoate (Figure 8B). A very slow decrease of the $\Delta\lambda$ ($A_I = 1.52$; $A_3 = 0.002$) was detected during the water rinse. However, a perturbation in the signal at the start of the water introduction suggests a fast rearrangement of the system at the sensor surface, with subsequent long relaxation to an equilibrium state. This finding suggests a different way of formation of the mixed system than using choline laurate (Figure 4) and choline decanoate (Figure 6) where the characteristic spike is not present.

The interactions of 200 mM choline octanoate with SVLs made of the natural lipids followed a different interaction pattern than with the SLB of egg PC (Figure 9). The characteristic feature of the $\Delta\lambda$ pattern is an initial exponential decrease during introduction of choline octanoate micelles, followed by a considerable increase in the $\Delta\lambda$ when the IL solution was changed for water. The mixed system stabilized at a $\Delta\lambda$ of 3 nm ($A_I = 3.14$ (yeast) and 3.19 (bovine liver)). Although fitting was not successful for *E. coli* SVL, the lowest $\Delta\lambda$ of the discussed mixed system was 2.5, which is slightly lower than with the other SVLs. The change from choline decanoate micelles to water showed a considerable increase in the $\Delta\lambda$ (1.8, 1.7, and 1.2 nm for *E. coli*, yeast, and bovine liver liposomes, respectively). This was the main difference between SVL and SLB interaction. In the case of *E. coli* and yeast SVL, the $\Delta\lambda$ remained stable after the increase while slow exponential decrease was observed with bovine liver SVL ($A_I = 3.61$; $A_3 = 0.010$).

The $\Delta\lambda$ analysis showed that removal of micelles caused an increased coverage of the sensor surface with the choline-octanoate-enriched system. Based on the obtained results, a possible explanation of the observed effect should be directly linked to the difference between the SLB and SVL, which lies in the ability of the intact vesicles to rupture and form a planar bilayer. Formation of a planar bilayer is connected to an increase in the $\Delta\lambda$, which is observed after choline octanoate micelle removal. Overall, the interaction with the natural lipid vesicles seems to proceed through the following steps: 1) the vesicles interact with choline octanoate micelles and the lipid bilayer is enriched with choline octanoate; 2) the whole system reaches equilibrium and the choline octanoate enriched vesicles are stabilized by interaction with micelles of choline octanoate; 3) removal of stabilizing micelles causes rupture of the adsorbed vesicles and a SLB from the choline octanoate/lipid mixture is formed. It was shown in our previous work that short chain phosphonium carboxylates caused malformation of zebrafish embryos [33]. There might be a connection with the presented results where the natural lipid membranes are not solubilized but their ability to stay in the vesicular form are compromised. Among the tested lipid extracts, the bovine liver lipid extract showed the lowest stability against the choline hexanoate micelles, and the system was still partially removed from the sensing surface after the formation of a SLB.

3.6 Interaction between choline hexanoate and lipid membranes

Due to the high CMC of choline hexanoate of 673 ± 2 mM [27], the choline hexanoate was present in the form of unimers in solution at the tested 200 mM concentration. Using a SLB of egg PC, the introduction of 200 mM

choline hexanoate induced an increase in the $\Delta\lambda$ of 0.6 nm (Figure 10A), and the $\Delta\lambda$ dropped 0.3 nm with water rinse. This data suggests that there is only little or no incorporation of choline hexanoate into the SLB of egg PC.

The introduction of 200 mM choline hexanoate onto immobilized SVL of *E. coli* liposomes increased the $\Delta\lambda$ by 1.1 nm (Figure 10B). Water rinse increased the $\Delta\lambda$ for further 0.5 nm. Such increase could be caused by either relaxation of the adsorbed vesicles, thus getting more in contact with the sensing surface. Or the second explanation speaks for the induction of SVL to SLB transformation. Formation of SLB seems to be more probable due to the high rate of the $\Delta\lambda$ increase. However, further analysis with complimentary methods would be necessary to support either of the hypotheses. Nevertheless, it seems that choline hexanoate is not able to solubilize phospholipid bilayer as was detected with choline laurate, choline decanoate and choline octanoate unimers.

The determined interaction of the SVL of yeast liposomes with choline hexanoate showed very low changes in peak shift (Figure 10C). This suggests that the yeast composition of the biomembrane is almost resistant to incorporation of choline hexanoate unimers and no considerable changes near the sensor surface are detected. The observed small fluctuations can be caused mainly by bulk liquids mixing between water and the concentrated solution of IL. The observed effect of choline hexanoate on the yeast in comparison to the *E. coli* could be partially explained by the high amount of ergosterol as the main sterol of fungi. The ratio of ergosterol to phospholipids can reach up to 3.31 in yeast plasmatic membrane but it is below 1 in the membranes of organelles [36]. In the total lipid extract the manufacturer states 54% to be unknown lipid species which could be to high extent occupied by ergosterols.

SVLs of bovine liver liposome did not show any change in $\Delta\lambda$ during choline hexanoate unimers introduction, however, a small exponential drop was observed with subsequent water rinse (Figure 10D). The parameters of the drop ($A_1 = 4.61$; $A_3 = 0.020$) suggest that new mixed system reached the equilibrium quickly. A cause of the drop could be destabilization of adsorption of part of the vesicles which was diminished as the IL was rinsed with water. The $\Delta\lambda$ drop also implies that bovine liver biomembranes are the most susceptible to the ILs even if not present in micellar form. Similar behavior of yeast lipid could again be connected to the content of cholesterol as 45% of lipid species was not identified, which correlates with a total ratio of cholesterol to phospholipids of 1 in animal cells.

The summary of the observed effects can be seen in Table 3. It confirms that the interaction grew stronger when longer chain ILs were applied, which correlates with the recently published studies of IL increasing alkyl chain length effect on the biomembranes [37,38]. However, each lipidic sensing platform demonstrated different susceptibility to a particular IL. The most probable reasons for such a change are differences between the lipid composition and the form of the supported biomembrane. Therefore, both of the factors need to be evaluated for an observed effect of IL or other membrane disrupting agents. It also shows that for biomimicking membranes studies the natural lipid membranes are beneficial due to provision of more relevant species-based information which would not be revealed using the simple biomembrane models, such as egg PC.

Table 3. Summary of the effect of increasing chain lengths in choline carboxylates on biomembranes composed of natural lipid extracts.

IL/biomembrane interaction effect summary table				
Supported lipid platform	IL concentration			
	200 mM choline hexanoate	200 mM choline octanoate	50 mM choline decanoate	20 mM choline laurate
egg PC SLB	-	++	++	+++
E. coli SVL	+	+	++	+++
Yeast SVL	-	++	++	++++
Liver SVL	+	++	++	+++
<p>LEGEND: +++++ very strong - complete removal of the SLB/SVL; +++ strong - the SLB/SVL compromised considerably; ++ moderate - approx. half of the original SLB/SVL signal observed; + slight – most of the SLB/SVL preserved on the surface; - no effect on the SLB/SVL observed</p>				

4 Conclusions

Natural lipids extracted from *E. coli*, yeast and bovine liver cells were successfully immobilized on SiO₂-coated sensors. The application of Ca-HEPES buffer allowed for rapid and stable adsorption of the heterogeneous lipid vesicles onto the sensor surface. The liposome immobilization procedure was monitored in real time by NPS. The data indicated that the liposomes were immobilized as intact vesicles in the form of a SVL in the case of *E. coli*, yeast and bovine liver liposomes, whereas a SLB was formed upon immobilization of egg PC liposomes.

The interactions between the immobilized liposomes (SLB and SVL) and choline carboxylates with four different alkyl chain lengths, including choline laurate, choline decanoate, choline octanoate and choline hexanoate, were further investigated. In general, the longer the alkyl chain, the stronger was the effect of the IL on the SLB and SVLs. This is well in accordance with the *Vibrio fischeri* toxicity studies showing an increase in toxicity upon an increase in the alkyl chain length. When the alkyl chain was shorter, higher concentrations were required to show the impact of the choline carboxylates on the liposomes. The effect observed with NPS generally followed the trend of toxicity of particular ILs, however the interactions of the studied ILs differed substantially for vesicles made of natural membrane extracts. We observed that yeast liposomes were the most sensitive to the introduction of choline laurate. The SVL of yeast liposome was completely disrupted and removed from the sensor surface after interaction with choline laurate. However, as the alkyl chain length got shorter, the SVL of bovine liver liposomes turn out to be the most sensitive towards the introduction of choline carboxylates. Choline hexanoate, which has the lowest cytotoxicity among the ILs studied in this work, was able to desorb part of the SVL of bovine liver liposomes. These results imply that the composition of the cell membrane plays a crucial role in its interaction with ILs. Therefore, to get a better understanding of the interaction between compounds and particular cell membranes, it is important to utilize natural lipid extracts and form biomimetic membranes, which closely mimic specific natural cell membranes.

Conflicts of interest

There are no conflicts to declare.

Acknowledgements

This work was supported by the Programme for research and mobility support of starting researchers of the Czech Academy of Sciences number MSM200311602 (F.D.) and by institutional support RVO:68081715 (F.D.). Academy of Finland (grant number 266342) is acknowledged for financial support (S.K.W). Financial support from Kemira Oyj is acknowledged (E.S. & A. W. T. K.).

5 References

- [1] A.L. Plant, M. Gueguetchkeri, W. Yap, Supported phospholipid/alkanethiol biomimetic membranes: insulating properties, *Biophys. J.* 67 (1994) 1126–1133. doi:10.1016/S0006-3495(94)80579-X.
- [2] H. Mozsolits, T.H. Lee, H.J. Wirth, P. Perlmutter, M.I. Aguilar, The interaction of bioactive peptides with an immobilized phosphatidylcholine monolayer, *Biophys. J.* 77 (1999) 1428–1444. doi:10.1016/S0006-3495(99)76991-2.
- [3] W. Hu, P.R. Haddad, K. Hasebe, M. Mori, K. Tanaka, M. Ohno, N. Kamo, Use of a biomimetic chromatographic stationary phase for study of the interactions occurring between inorganic anions and phosphatidylcholine membranes, *Biophys. J.* 83 (2002) 3351–3356. doi:10.1016/S0006-3495(02)75335-6.
- [4] R.L. Owen, J.K. Strasters, E.D. Breyer, Lipid vesicles in capillary electrophoretic techniques: Characterization of structural properties and associated membrane-molecule interactions, *Electrophoresis.* 26 (2005) 735–751. doi:10.1002/elps.200410288.
- [5] J.M. Dabkowski, M. Muthukumar, E.B. Coughlin, J.G. Pool, A. Som, G.J. Gabriel, G.N. Tew, Interactions between Antimicrobial Polynorbornenes and Phospholipid Vesicles Monitored by Light Scattering and Microcalorimetry, *Langmuir.* 24 (2008) 12489–12495. doi:10.1021/la802232p.
- [6] J. Witos, G. Russo, S.-K. Ruokonen, S.K. Wiedmer, Unraveling Interactions between Ionic Liquids and Phospholipid Vesicles Using Nanoplasmonic Sensing, *Langmuir.* 33 (2017) 1066–1076. doi:10.1021/acs.langmuir.6b04359.
- [7] N.J. Cho, J.A. Jackman, M. Liu, C.W. Frank, PH-driven assembly of various supported lipid platforms: A comparative study on silicon oxide and titanium oxide, *Langmuir.* 27 (2011) 3739–3748. doi:10.1021/la104348f.
- [8] A. Åkesson, T. Lind, N. Ehrlich, D. Stamou, H. Wacklin, M. Cárdenas, Composition and structure of mixed phospholipid supported bilayers formed by POPC and DPPC, *Soft Matter.* 8 (2012) 5658–5665. doi:10.1039/c2sm00013j.
- [9] A. Olżyńska, M. Zubek, M. Roeselova, J. Korchowiec, L. Cwiklik, Mixed DPPC/POPC Monolayers: All-atom Molecular Dynamics Simulations and Langmuir Monolayer Experiments, *Biochim. Biophys. Acta - Biomembr.* 1858 (2016) 3120–3130. doi:10.1016/j.bbamem.2016.09.015.
- [10] J. Yang, J. Martí, C. Calero, Pair interactions among ternary DPPC/POPC/cholesterol mixtures in liquid-ordered and liquid-disordered phases, *Soft Matter.* 12 (2016) 4557–4561. doi:10.1039/c6sm00345a.
- [11] G. Russo, J. Witos, A.H. Rantamäki, S.K. Wiedmer, Cholesterol affects the interaction between an ionic liquid and phospholipid vesicles. A study by differential scanning calorimetry and nanoplasmonic sensing, *Biochim. Biophys. Acta - Biomembr.* 1859 (2017) 2361–2372. doi:10.1016/j.bbamem.2017.09.011.
- [12] F. Duša, W. Chen, J. Witos, S.K. Wiedmer, Calcium Dependent Reversible Aggregation of Escherichia coli Biomimicking Vesicles Enables Formation of Supported Vesicle Layers on Silicon Dioxide, *Front. Mater.* 6 (2019) 1–8. doi:10.3389/fmats.2019.00023.
- [13] J.T. Hautala, M. V. Lindén, S.K. Wiedmer, S.J. Ryhänen, M.J. Säily, P.K.J. Kinnunen, M.L. Riekkola, Simple coating of capillaries with anionic liposomes in capillary electrophoresis, *J. Chromatogr. A.* 1004 (2003) 81–90. doi:10.1016/S0021-9673(03)00570-3.
- [14] S.K. Wiedmer, M. Jussila, R.M.S. Hakala, K.H. Pystynen, M.L. Riekkola, Piperazine-based buffers for liposome coating of capillaries for electrophoresis, *Electrophoresis.* 26 (2005) 1920–1927. doi:10.1002/elps.200410277.
- [15] K. Ninomiya, T. Yamauchi, M. Kobayashi, C. Ogino, N. Shimizu, K. Takahashi, Cholinium carboxylate ionic liquids for pretreatment of lignocellulosic materials to enhance subsequent enzymatic saccharification, *Biochem. Eng. J.* 71 (2013) 25–29. doi:10.1016/j.bej.2012.11.012.
- [16] A. Xu, X. Guo, Y. Zhang, Z. Li, J. Wang, Efficient and sustainable solvents for lignin dissolution: Aqueous choline carboxylate solutions, *Green Chem.* 19 (2017) 4067–4073. doi:10.1039/c7gc01886j.
- [17] K.S. Egorova, V.P. Ananikov, Toxicity of Ionic Liquids: Eco(cyto)activity as Complicated, but Unavoidable Parameter for Task-Specific Optimization, *ChemSusChem.* 7 (2014) 336–360. doi:10.1002/cssc.201300459.

- [18] S.K. Mikkola, A. Robciuc, J. Lokajová, A.J. Holding, M. Lämmerhofer, I. Kilpeläinen, J.M. Holopainen, A.W.T. King, S.K. Wiedmer, Impact of amphiphilic biomass-dissolving ionic liquids on biological cells and liposomes, *Environ. Sci. Technol.* 49 (2015) 1870–1878. doi:10.1021/es505725g.
- [19] A.H. Rantamäki, S.K. Ruokonen, E. Sklavounos, L. Kyllönen, A.W.T. King, S.K. Wiedmer, Impact of surface- active guanidinium-, tetramethylguanidinium-, and cholinium-based ionic liquids on vibrio Fischeri cells and dipalmitoylphosphatidylcholine liposomes, *Sci. Rep.* 7 (2017) 1–12. doi:10.1038/srep46673.
- [20] D. Rengstl, B. Kraus, M. Van Vorst, G.D. Elliott, W. Kunz, Effect of choline carboxylate ionic liquids on biological membranes, *Colloids Surfaces B Biointerfaces.* 123 (2014) 575–581. doi:10.1016/j.colsurfb.2014.09.057.
- [21] K.A. Willets, R.P. Van Duyne, Localized Surface Plasmon Resonance Spectroscopy and Sensing, *Annu. Rev. Phys. Chem.* 58 (2007) 267–297. doi:10.1146/annurev.physchem.58.032806.104607.
- [22] G.A. Lopez, M.-C.C. Estevez, M. Soler, L.M. Lechuga, Recent advances in nanoplasmonic biosensors: Applications and lab-on-a-chip integration, *Nanophotonics.* 6 (2017) 123–136. doi:10.1515/nanoph-2016-0101.
- [23] M. Citartan, S.C.B. Gopinath, J. Tominaga, T.-H. Tang, Label-free methods of reporting biomolecular interactions by optical biosensors, *Analyst.* 138 (2013) 3576. doi:10.1039/c3an36828a.
- [24] M.P. Jonsson, P. Jönsson, A.B. Dahlin, F. Höök, Supported lipid bilayer formation and lipid-membrane-mediated biorecognition reactions studied with a new nanoplasmonic sensor template., *Nano Lett.* 7 (2007) 3462–8. doi:10.1021/nl072006t.
- [25] E. Oh, J.A. Jackman, S. Yorulmaz, V.P. Zhdanov, H. Lee, N.J. Cho, Contribution of temperature to deformation of adsorbed vesicles studied by nanoplasmonic biosensing, *Langmuir.* 31 (2015) 771–781. doi:10.1021/la504267g.
- [26] J.A. Jackman, B. Špačková, E. Linardy, M.C. Kim, B.K. Yoon, J. Homola, N.-J. Cho, Nanoplasmonic ruler to measure lipid vesicle deformation., *Chem. Commun. (Camb).* 52 (2016) 76–79. doi:10.1039/c5cc06861d.
- [27] S.K. Ruokonen, C. Sanwald, A. Robciuc, S. Hietala, A.H. Rantamäki, J. Witos, A.W.T. King, M. Lämmerhofer, S.K. Wiedmer, Correlation between Ionic Liquid Cytotoxicity and Liposome–Ionic Liquid Interactions, *Chem. - A Eur. J.* 24 (2018) 2669–2680. doi:10.1002/chem.201704924.
- [28] F. Duša, W. Chen, J. Witos, S.K. Wiedmer, Nanoplasmonic Sensing and Capillary Electrophoresis for Fast Screening of Interactions between Phosphatidylcholine Biomembranes and Surfactants, *Langmuir.* 34 (2018) 5889–5900. doi:10.1021/acs.langmuir.8b01074.
- [29] <http://www.kyenslab.com/en/index.html>, (n.d.).
- [30] J.A. Jackman, V.P. Zhdanov, N.J. Cho, Nanoplasmonic biosensing for soft matter adsorption: Kinetics of lipid vesicle attachment and shape deformation, *Langmuir.* 30 (2014) 9494–9503. doi:10.1021/la502431x.
- [31] M. Dacic, J.A. Jackman, S. Yorulmaz, V.P. Zhdanov, B. Kasemo, N.-J.J. Cho, Influence of divalent cations on deformation and rupture of adsorbed lipid vesicles, *Langmuir.* 32 (2016) 6486–6495. doi:10.1021/acs.langmuir.6b00439.
- [32] G.H. Zan, J.A. Jackman, S.O. Kim, N.J. Cho, Controlling lipid membrane architecture for tunable nanoplasmonic biosensing, *Small.* 10 (2014) 4828–4832. doi:10.1002/sml.201400518.
- [33] S.-K. Ruokonen, C. Sanwald, M. Sundvik, S. Polnick, K. Vyavaharkar, F. Duša, A.J. Holding, A.W.T. King, I. Kilpeläinen, M. Lämmerhofer, P. Panula, S.K. Wiedmer, Effect of Ionic Liquids on Zebrafish (*Danio rerio*) Viability, Behavior, and Histology; Correlation between Toxicity and Ionic Liquid Aggregation, *Environ. Sci. Technol.* 50 (2016) 7116–7125. doi:10.1021/acs.est.5b06107.
- [34] O. López, A. De La Maza, L. Coderch, C. López-Iglesias, E. Wehrli, J.L. Parra, Direct formation of mixed micelles in the solubilization of phospholipid liposomes by Triton X-100, *FEBS Lett.* 426 (1998) 314–318. doi:10.1016/S0014-5793(98)00363-9.
- [35] S.-K. Ruokonen, F. Duša, J. Lokajová, I. Kilpeläinen, A.W.T. King, S.K. Wiedmer, Effect of ionic liquids on the interaction between liposomes and common wastewater pollutants investigated by capillary electrophoresis, *J. Chromatogr. A.* 1405 (2015) 178–187. doi:10.1016/j.chroma.2015.05.064.

- [36] E. Zinser, C.D.M. Sperka-Gottlieb, E. V. Fasch, S.D. Kohlwein, F. Paltauf, G. Daum, Phospholipid synthesis and lipid composition of subcellular membranes in the unicellular eukaryote *Saccharomyces cerevisiae*, *J. Bacteriol.* 173 (1991) 2026–2034. doi:10.1128/jb.173.6.2026-2034.1991.
- [37] S. Kumar, H.A. Scheidt, N. Kaur, T.S. Kang, G.K. Gahlay, D. Huster, V.S. Mithu, Effect of the Alkyl Chain Length of Amphiphilic Ionic Liquids on the Structure and Dynamics of Model Lipid Membranes, *Langmuir.* 35 (2019) 12215–12223. doi:10.1021/acs.langmuir.9b02128.
- [38] K. Cook, K. Tarnawsky, A.J. Swinton, D.D. Yang, A.S. Senetra, G.A. Caputo, B.R. Carone, T.D. Vaden, Correlating Lipid Membrane Permeabilities of Imidazolium Ionic Liquids with their Cytotoxicities on Yeast, Bacterial, and Mammalian Cells, *Biomolecules.* 9 (2019) 23–29. doi:10.3390/biom9060251.

Figure captions

Figure 1. Structures of the studied choline carboxylates, including choline laurate, choline decanoate, choline octanoate, and choline hexanoate.

Figure 2. Immobilization of liposomes: (A) SLB of egg PC, (B) SVL of *E. coli*, (C) SVL of yeast, and (D) SVL of bovine liver liposomes, monitored by NPS.

Figure 3. Blank (reference) values of choline carboxylates on the SiO₂ sensor: (A) 20 mM of choline laurate, (B) 50 mM of choline decanoate, (C) 200 mM of choline octanoate, and (D) 200 mM of choline hexanoate.

Figure 4. Interaction between SLB of egg PC and choline laurate at different concentrations: (a) 0.5 mM, (b) 5 mM, and (c) 20 mM of choline laurate.

Figure 5. Interaction between 20 mM choline laurate and three different SVL made of natural lipid extracts: (A) *E. coli*, (B) yeast, and (C) bovine liver lipid extracts.

Figure 6. Interactions between SLBs of egg PC and choline decanoate at different concentrations: (A) 20 mM, (B) 50 mM, and (C) 105 mM of choline decanoate.

Figure 7. Interactions between 50 mM of choline decanoate and three different SVLs made of natural lipids extracts: (A) *E. coli*, (B) yeast, and (C) bovine liver lipid extracts.

Figure 8. Interaction between egg PC SLBs and choline octanoate at a concentration of (A) 50 mM and (B) 200 mM of choline octanoate.

Figure 9. Interactions between 200 mM of choline octanoate and SVLs made of lipids extracted from (A) *E. coli*, (B) yeast, and (C) bovine liver lipid.

Figure 10. Interactions between 200 mM choline hexanoate and lipid membrane made of lipids extracts from (A) egg PC, (B) *E. coli*, (C) yeast, and (D) bovine liver.